Spin control of light with hyperbolic metasurfaces

Oleh Y. Yermakov,[1,*] Anton I. Ovcharenko,[1] Andrey A. Bogdanov,[1] Ivan V. Iorsh,[1]
Konstantin Y. Bliokh,[2,3] and Yuri S. Kivshar[1,3]
[1]*ITMO University, St. Petersburg 197101, Russia*
[2]*Center for Emergent Matter Science, RIKEN, Wako-shi, Saitama 351-0198, Japan*
[3]*Nonlinear Physics Centre, Research School of Physics and Engineering, Australian National University, Canberra ACT 2601, Australia*
(Received 24 May 2016; revised manuscript received 14 August 2016; published 31 August 2016)

Transverse spin angular momentum is an inherent feature of evanescent waves which may have applications in nanoscale optomechanics, spintronics, and quantum information technology due to the robust spin-directional coupling. Here we analyze local spin angular momentum density of hybrid surface waves propagating along anisotropic hyperbolic metasurfaces. We reveal that, in contrast to bulk plane waves and conventional surface plasmons at isotropic interfaces, the spin of the hybrid surface waves can be engineered to have an arbitrary angle with the propagation direction. This property allows us to tailor directivity of surface waves via the magnetic control of the spin projection of quantum emitters, and it can be useful for optically controlled spin transfer.

DOI: 10.1103/PhysRevB.94.075446

I. INTRODUCTION

Metasurfaces are artificial two-dimensional nanostructured materials which exhibit new properties allowing one to control and manage light propagation in an unusual way [1]. Recently, there has been significant interest in metasurfaces [2,3], which is related to the interesting features and advantages that can be offered by these structures [4]. Keeping the rich functionality of three-dimensional metamaterials, metasurfaces are simpler to fabricate, and they can be easily integrated into on-chip optical devices [5–7]. Metasurfaces provide efficient beam shaping, phase, and polarization control of light allowing construction of virtually arbitrary polarization vectors of the reflected or transmitted waves [8–14].

Another appealing feature of metasurfaces is that, similarly to bulk metamaterials providing efficient control over the bulk modes, metasurfaces provide an unprecedented control over dispersion and polarization of surface waves [15–18]. This idea was put forward in the seminal paper [19] in application to graphene metasurfaces and was recently realized experimentally in the visible frequency range with the plasmonic grating structure [20]. Namely, a negative refraction of surface plasmon-polaritons has been demonstrated at the *hyperbolic metasurface*, representing as silver/air grating with appropriate sub-wavelength sizes [20], i.e., a system characterized by the surface conductivity tensor with the principal components having different signs [21–24].

It has been pointed out that the directivity of surface plasmons at the hyperbolic metasurfaces can be controlled with high flexibility, allowing almost unidirectional propagation of surface waves excited by a point source. Recently, it was also shown [25–31] that evanescent waves exhibit robust transverse coupling between their spin angular momentum and propagation direction. In this work we show that a hyperbolic metasurface provides highly tunable spin-directional coupling. It results in the directional excitation of the surface waves in the case of a rotating dipole placed in the vicinity of the optical interface.

The studies of surface waves have recently gained a new feature, since it was shown that they possess the unusual *transverse spin angular momentum*, perpendicular to their propagation direction [32,33]. Transverse spin is a generic feature of inhomogeneous light fields, and it has recently attracted considerable attention [26,27]. It is important to mention that a number of recent experiments [25,28–30] demonstrated that the transverse spin of evanescent waves provides a robust spin-direction coupling in a variety of optical systems [31]. Both transfer and control over the angular momentum of light at the nanoscale have a plethora of perspective applications in nanoscaled optomechanics [34–37], paving a way towards multidirectional mechanical control of nanoobjects with light. Moreover, the coupling of the surface waves carrying the angular momentum to the magnetic solid state system leads to novel magneto-optical phenomena such as the transversal magneto-optical Kerr effect [38], and it opens new perspectives for the efficient optical control over the spin currents in solid state systems, which is a subject of the rapidly emerging field of *spinoptronics*. As such, it offers an efficient tool for spin-dependent control of light [39].

Electromagnetic eigenmodes of free space are *plane waves* whose spectrum (light cone) is double degenerate with respect to polarization degrees of freedom. The spin angular momentum of a plane wave is always collinear to the propagation direction, and its projection on the wave vector (i.e., helicity) lies in the range $[-1,1]$. The helicity eigenmodes are left-handed and right-handed circularly polarized waves. Note that here and in what follows we consider pure momentum eigenmodes; superpositions of plane waves have more sophisticated spin properties [26,27].

Electromagnetic *surface waves* can appear, e.g., at an interface between two isotropic media. In the generic case, the spectrum of surface waves is nondegenerate, and either linear TM or linear TE modes exist. For TM (TE) modes, the electric (magnetic) field rotates in the plane perpendicular to the interface and containing the wave vector. Therefore, spin of surface waves lies in the plane of the interface and is directed perpendicularly to the wave vector, in contrast to bulk plane waves [31]. Thus, in isotropic media, the spin angular momentum can be either purely longitudinal for plane waves

*o.yermakov@phoi.ifmo.ru

or purely transverse for surface waves. For nanophotonic applications, it would nevertheless be desirable to be able to tune spin direction and its absolute value continuously.

In this work we reveal that surface waves localized at *anisotropic* metasurfaces can serve as an instrument to bridge this gap. We show that polarization of such surface waves can continuously change from linear TE or TM to elliptical, or circular (left of right) as a particular case. It provides controllable change of the angle between the spin and propagation direction in the range from 0 to π. These findings open new routes for both optomechanical manipulation of nanoobjects and for optical control over spin transport in semiconductor nanostructures coupled to hyperbolic metasurfaces.

II. DISPERSION OF HYBRID SURFACE WAVES

We consider a two-dimensional anisotropic structure shown in Fig. 1(a). Specific realizations include natural two-dimensional anisotropic materials such as hexagonal boron nitride [40–42], plasmonic gratings of different geometries [43,44], or patterned graphene nanostructures [23,45]. For microwaves, such anisotropic metasurfaces can be realized with LC circuits contours [46].

Within the local approximation the electromagnetic response of an anisotropic metasurface can be characterized by a surface conductivity tensor [3]:

$$\widehat{\sigma}_0 = \begin{pmatrix} \sigma_\perp & 0 \\ 0 & \sigma_\parallel \end{pmatrix}. \tag{1}$$

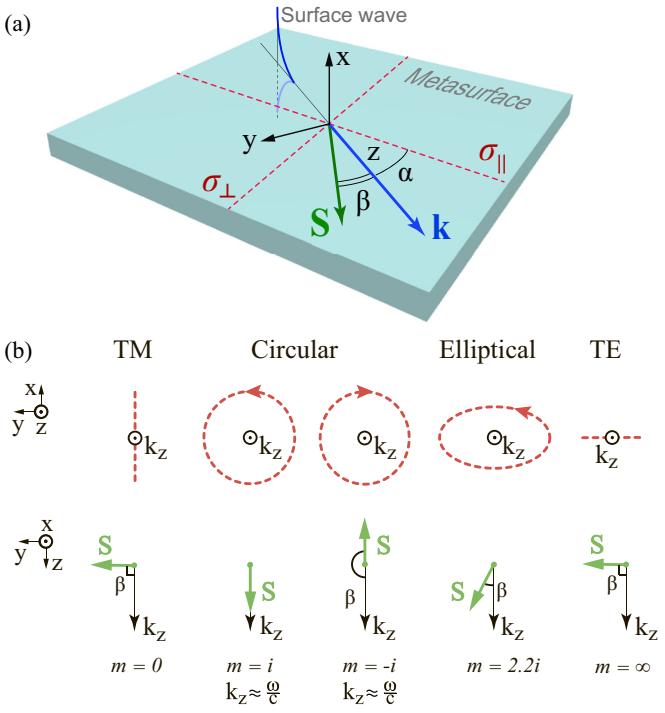

FIG. 1. (a) Geometry of the structure. (b) Polarization of hyperbolic plasmons for different polarization parameters m [see Eq. (7)] with corresponding angles β between plasmon propagation and spin angular momentum. The red arrow shows the direction of the electric field vector rotation.

We assume that conductivity tensor components have a resonance behavior described by the Drude-Lorentz approximation:

$$\sigma_s(\omega) = A_s \frac{ic}{4\pi} \frac{\omega}{\omega^2 - \Omega_s^2 + i\gamma_s\omega}, \quad s = \perp, \parallel. \tag{2}$$

Here A_s is a constant, which depends on design, Ω_s is the resonant frequency, and γ_s is the bandwidth of the resonance defined by losses. For the sake of simplicity, hereinafter we neglect losses, $\gamma_s = 0$, chose A_s equal to 1, and assume that $\Omega_\perp < \Omega_\parallel$. Three dispersion regimes of the metasurface can be distinguished depending on the signature of the conductivity tensor (1): (i) a capacitive regime at $\omega < \Omega_\perp$ when $\mathrm{Im}(\sigma_\perp) < 0$ and $\mathrm{Im}(\sigma_\parallel) < 0$; (ii) an inductive regime at $\omega > \Omega_\parallel$ when $\mathrm{Im}(\sigma_\perp) > 0$ and $\mathrm{Im}(\sigma_\parallel) > 0$; and a hyperbolic regime at $\Omega_\perp < \omega < \Omega_\parallel$ when $\mathrm{Im}(\sigma_\perp)\mathrm{Im}(\sigma_\parallel) < 0$ by an analogy with bulk metamaterials where permittivity tensor components have different signs [47,48].

The dispersion equation for surface waves propagating along the z axis rotated by an angle α with respect to the $\parallel$ direction [see Fig. 1(a)] is given by [22]

$$\left(\frac{\kappa}{k_0} - \frac{2\pi i}{c}\sigma_{yy}\right)\left(\frac{k_0}{\kappa} + \frac{2\pi i}{c}\sigma_{zz}\right) = \frac{4\pi^2}{c^2}\sigma_{yz}^2, \tag{3}$$

$$\sigma_{yy,zz} = \bar{\sigma} \mp \delta\sigma \cos(2\alpha),$$
$$\sigma_{yz} = \sigma_{zy} = \delta\sigma \sin(2\alpha). \tag{4}$$

Here we use the following notations: $\bar{\sigma} = (\sigma_\perp + \sigma_\parallel)/2$, $\delta\sigma = (\sigma_\parallel - \sigma_\perp)/2$, $k_0 = \omega/c$, and $\kappa = \sqrt{k_z^2 - k_0^2}$.

Angle α is the main parameter, which determines the propagation direction of the surface waves with respect to the anisotropy axis of the metasurface. It defines the relationship between the anisotropic properties of the metasurface and polarization (spin) properties of surface modes. When $\alpha = \pi n/2$ (n is an integer number), the wave propagates along one of the anisotropy axes of the metasurface. In this case, the right-hand side of Eq. (3) vanishes and the dispersion equation factorizes into two independent equations corresponding to the pure TE mode (left brackets) and the pure TM mode (right brackets). Straightforward analysis of Eq. (3) shows that (i) in the low-frequency (capacitive) regime the only TE mode is localized, (ii) in the high frequency (inductive) regime the only TM mode is localized, and (iii) in the hyperbolic regime simultaneous propagation of both modes is possible.

It should be mentioned that, at a microscopic scale comparable with size of the unit cell, polarization of the electromagnetic field is hybrid. However, in our work the polarization is hybrid globally, i.e., after averaging the electromagnetic field over the unit cell. In particular, a point emitter feels the microscopic field, but, if its size is much larger than a unit cell and smaller than a wavelength, one can describe their interaction within an effective medium approach.

It is reasonable to refer to the surface waves under consideration as *two-dimensional Dyakonov plasmons* since they have a hybrid polarization structure and dispersion, which depends on the propagation direction. However, in contrast to the conventional Dyakonov waves [49,50], which propagate along a plane interface separating isotropic and anisotropic

bulk materials, the spectrum of the analyzed surface waves consists of two branches (TE and TM), and both of them can propagate in the isotropic case when a metasurface is described by a scalar conductivity. Moreover, the surface modes at an anisotropic metasurface are more localized and have a much wider range of propagation angles.

For oblique propagation $\alpha \neq \pi n/2$, two linear polarizations get mixed and, strictly speaking, no specific linear polarization can be assigned to the eigenmodes of the structure. However, for brevity, further on we will denote the upper frequency mode as a *quasi-TM* surface wave and the lower frequency one as *quasi-TE*.

The quasi-TE mode has no frequency cutoff, but has an angular-dependent resonant frequency $\omega_r^2 = \Omega_\parallel^2 \sin^2(\alpha) + \Omega_\perp^2 \cos^2(\alpha)$ for which $k_z(\omega_r) \to \infty$ [see Figs. 2(a), 2(c), and 2(e)]. The quasi-TM mode can propagate at an arbitrary high frequency but has an angular-dependent frequency cutoff $\omega_c^2 = \Omega_\parallel^2 \cos^2(\alpha) + \Omega_\perp^2 \sin^2(\alpha)$ [see Figs. 2(a), 2(c), and 2(e)].

III. SPIN ANGULAR MOMENTUM OF HYBRID SURFACE WAVES

The spin angular momentum of a monochromatic electromagnetic field has intrinsic nature and is described by the local spin density. It should be noticed that total spin angular momentum of surface waves vanishes due to the symmetry of the problem. Total nonzero spin angular momentum can be revealed when permittivities of sub- and superstrate are different. However, in many practical problems, local light-matter interactions (e.g., with atoms, nanoparticles, or quantum dots) are typically sensitive to the *local* spin density, in particular to its *electric* part [25,26,28–30,51], which usually has more sophisticated x-dependent properties than the total spin [26]. Here and in what follows we will investigate the local spin density, which is a fundamental spin characteristic of surface modes, and we will denote it as *spin angular momentum* for brevity.

For surface waves, localized along the x axis, we determine the local spin density normalized per "one photon" in units $\hbar = 1$ as [33,52]:

$$\mathbf{S} = \frac{\mathrm{Im}[\mathbf{E}^* \times \mathbf{E} + \mathbf{H}^* \times \mathbf{H}]}{W}, \tag{5}$$

where $W = |\mathbf{E}|^2 + |\mathbf{H}|^2$ characterizes the local energy density of the field. The dependence on the coordinates is excluded due to the normalization by the local energy density in Eq. (5).

In general case, we can express the electromagnetic fields through the polarization parameter m in this way:

$$\mathbf{E} = \left(\pm 1, m\frac{k_0}{k_z}, -i\frac{\kappa}{k_z}\right) e^{ik_z z - \kappa|x|},$$
$$\mathbf{H} = \left(-m, \pm\frac{k_0}{k_z}, \pm im\frac{\kappa}{k_z}\right) e^{ik_z z - \kappa|x|}. \tag{6}$$

Sign "+" corresponds to the upper half-space and "−" to the lower one.

To analyze the spin angular momentum of the surface waves supported by the anisotropic metasurface, we consider the upper half-space. Substituting electric and magnetic fields of surface modes at the anisotropic metasurface [Eq. (6)] into

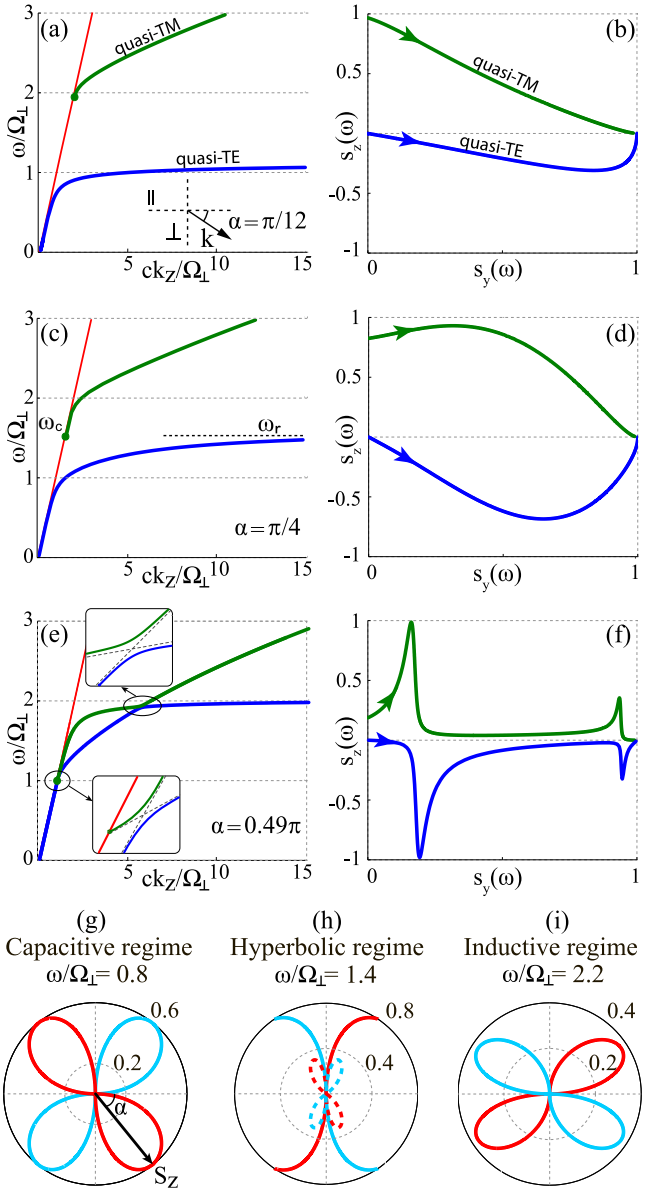

FIG. 2. Dispersion of the surface waves [(a), (c), and (e)] and corresponding parametric plots of spin angular momentum [(b), (d), and (f)] for quasi-TE (blue lines) and quasi-TM (green lines) modes for different propagation angles ($\alpha = \pi/12, \pi/4, 0.49\pi$). The red lines in figures (a), (c), and (e) show the light line. The arrows in figures (b), (d), and (f) correspond to the frequency augmentation. (g)–(i) Dependence of longitudinal spin angular momentum S_z on propagation direction α in polar coordinates for different frequencies $\omega/\Omega_\perp = 0.8, 1.4, 2.2$. Red color corresponds to the positive sign and cyan to the negative one. In (h) solid lines correspond to quasi-TM mode and dashed lines to quasi-TE mode.

Eq. (5), we arrive at the following expression:

$$\mathbf{S} = \left(0, \frac{\kappa}{k_z}, \frac{2\mathrm{Im}(m)}{1+|m|^2}\frac{k_0}{k_z}\right), \quad m = \frac{\frac{2\pi}{c}\sigma_{yz}}{1 - i\frac{2\pi k_0}{\kappa c}\sigma_{yy}}. \tag{7}$$

Here the complex polarization parameter m is defined by the structure of the conductivity tensor in the surface waves, while for the plane waves m represents just a ratio of the transverse

electric-field components E_y/E_x [26,33]. Equation (7) is the central analytical result of our work, which describes the local spin angular momentum density of surface electromagnetic modes at anisotropic metasurfaces.

It is important to mention that in the isotropic case, $\sigma_\perp = \sigma_\parallel = \bar{\sigma}$ and $\delta\sigma = 0$, when the conductivity tensor (1) is scalar, only pure TM ($m = 0$) and TE ($m = \infty$) surface modes exist. This case corresponds, for example, to *graphene plasmons* [53]. Equation (7) shows that graphene plasmons carry purely transverse spin $\mathbf{S} = (0,\kappa/k_z,0)$ independently of the material properties.

For anisotropic metasurfaces, parameter m can take on arbitrary values. Then, the surface modes are elliptically polarized, and their spin angular momentum is rotated by an angle β with respect to the propagation direction, as shown in Fig. 1(b). Special cases of $m = \pm i$ correspond to right-hand and left-hand circularly polarized waves [with $\kappa \ll k_z \simeq k_0$ and almost longitudinal spin $\mathbf{S} \simeq (0,0,\pm 1)$], whereas the $m = 0$ and $m = \infty$ cases correspond to TM or TE modes [with purely transverse spin $\mathbf{S} = (0,\kappa/k_z,0)$]. All intermediate cases with the arbitrary spin direction (within the metasurface plane) can be realized for the surface waves under consideration.

Pure TE and TM surface modes appear for $\alpha = \pi n/2$. For the oblique propagation $\alpha \neq \pi n/2$, quasi-TE and quasi-TM modes are elliptically polarized and have nonzero longitudinal and transverse spin components. The evolution of these components (S_z and S_y) along the dispersion curves of the quasi-TE and quasi-TM surface waves for different propagation angles ($\alpha = \pi/12, \pi/4, 0.49\pi$) are shown in Figs. 2(b), 2(d), and 2(f). The corresponding dispersion curves of the surface waves are shown in Figs. 2(a), 2(c), and 2(e). The longitudinal spin component of the quasi-TM mode can change from 1 [see Fig. 2(b)] in the vicinity of frequency cutoff to 0 at high frequencies, whereas the longitudinal spin of the quasi-TE approaches zero for both small and large k_z.

Comparison of Figs. 2(b) and 2(d) shows that the hybridization is stronger when the propagation direction becomes farther from the the principal axes. So, at $\alpha = \pi/4$, it results in relatively large longitudinal spin S_z for the quasi-TE mode. For the quasi-TM mode S_z approaches 1 at some finite k_z, but does not reach it.

In the hyperbolic regime of the metasurface, simultaneous propagation of two modes is possible. For $\alpha = \pm\pi/2$, the dispersion curves of the TE and TM modes with purely transverse spin crosses; i.e., an *accidental degeneracy* takes place. Small deviation of α from $\pm\pi/2$ lifts the degeneracies, and anticrossing gaps open [see Fig. 2(e)]. The anticrossings signify the *hybridization* of the TE and TM modes. This brings about sharp resonances in the longitudinal spin components [Fig. 2(f)]. In these resonances, hybridized surface eigenmodes acquire circular polarizations and can posses nearly longitudinal spin. This is in contrast to the usual surface waves with purely transverse spin.

Notably, the quasi-TE and quasi-TM modes always have transverse spins of the same sign and longitudinal spins of the opposite signs. The dependences of S_z on α for three different dispersion regimes of metasurface is shown in Figs. 2(g), 2(h), and 2(i). For the quasi-TE mode, $S_z < 0$ when α lies in the first and third quadrants and $S_z > 0$ in the second and forth quadrants. For the quasi-TM modes, the situation is reversed.

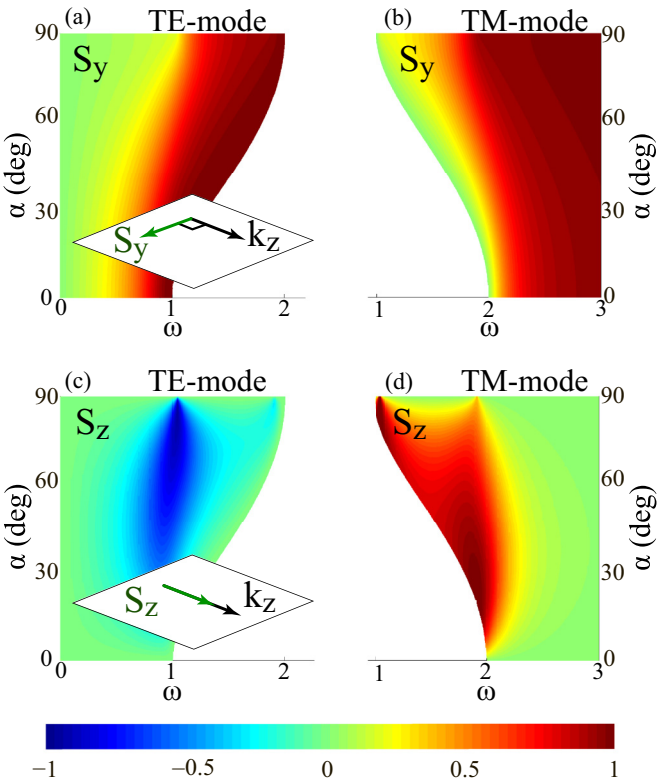

FIG. 3. Spin angular momentum isocurves as functions of frequency ω and propagation angle α for the transverse component of spin angular momentum for TE (a) and for TM (b) modes, and for the longitudinal component of spin angular momentum for TE (c) and for TM (d) modes.

Note that for the quasi-TM mode in the hyperbolic regime the contours are open [Fig. 2(h)]. It happens due to the hyperbolic shape of the equal frequency contours, which forbids the propagation of the surface wave in certain range of angles.

Comprehensive information about angular and frequency dependences of the transverse (S_y) and longitudinal (S_z) spin components for quasi-TE and quasi-TM modes is provided in Fig. 3. As discussed previously, the transverse spin increases monotonically with frequency for a fixed propagation direction for both modes. At the same time, the longitudinal spin behavior depends crucially on the propagation direction α. When $\alpha \to \pi/2$ one can see two resonances both for quasi-TM and quasi-TE modes, which are also seen in Fig. 2(f).

Essentially, there are two mechanisms of the hybridization of surface TE and TM modes, which determine their spin angular momenta: (i) smooth anisotropy-induced hybridization of modes into quasi-TE and quasi-TM eigenmodes and (ii) resonant hybridization due to an accidental degeneracy of the eigenmodes in the hyperbolic regime.

The peculiar properties of spin-orbit coupling in anisotropic metasurface are expected to have a pronounced effect on the dynamics of quantum many-body systems such as two-dimensional arrays of quantum dots coupled to such structures. Specifically, if a pair of quantum emitters is placed on top of the metasurface, they would interact via emission and reabsorption of surface waves supported by the metasurface. Due to the spin-locking of surface waves, this interaction

will naturally depend on the spin projections of the quantum emitters and, generally speaking, it will be asymmetric; i.e., the excitation transfer rate in one direction will be larger than that in the opposite direction. Remarkably, one-dimensional arrays of quantum emitters placed on top of plasmonic surfaces and quasi-one-dimensional waveguides, where one-dimensional spin-orbit coupling is present, have recently attracted sufficient research interest [54], and they appear to be a suitable platform for the realization of novel quantum protocols for quantum information processing [55]. Moreover, chains of quantum emitters place into waveguides demonstrate a plethora of interesting fundamental phenomena such as chiral quantum walks [56] and unconventional phase transitions.

Thus, anisotropic metasurfaces can naturally extend the field of chiral quantum optics into two dimensions. The dynamics of the arrays of quantum emitters placed on a metasurface should be treated within the master equation for the density matrix approach, and it remains the subject of the ongoing work.

IV. CONCLUSION

We have analyzed the spin angular momentum of surface waves localized at anisotropic metasurfaces. We have shown that hyperbolic metasurfaces allow flexible control of both longitudinal and transverse components of the spin angular momentum of surface waves. This finding is in a sharp contrast to the properties of conventional surface waves localized at interfaces of isotropic materials, which carry purely transverse spin. Two-dimensional tunability of optical spin at anisotropic interfaces can enrich considerably various spin-orbit interaction phenomena, which currently attract enormous attention in nanophotonics and near-field optics [25,28–31,39], forming a new direction of spin-orbit photonics [57].

ACKNOWLEDGMENTS

This work was supported by RFBR (16-37-60064, 15-32-20665, 14-02-01223), the President of the Russian Federation (MK-6462.2016.2), the program of Fundamental Research in Nanotechnology and Nanomaterials of the Russian Academy of Science, and the Australian Research Council. Numerical simulations have been supported by the Russian Science Foundation (Grant No. 15-12-20028).

[1] N. Yu and F. Capasso, Nat. Mater. **13**, 139 (2014).
[2] N. Yu and F. Capasso, J. Lightwave Technol. **33**, 2344 (2015).
[3] S. B. Glybovski, S. A. Tretyakov, P. A. Belov, Y. S. Kivshar, and C. R. Simovski, Phys. Rep. **634**, 1 (2016).
[4] C. L. Holloway, E. F. Kuester, J. Gordon, J. O. Hara, J. Booth, and D. R. Smith, IEEE Antennas Propag. Mag. **54**, 10 (2012).
[5] A. V. Kildishev, A. Boltasseva, and V. M. Shalaev, Science **339**, 1232009 (2013).
[6] C. Wu, N. Arju, G. Kelp, J. A. Fan, J. Dominguez, E. Gonzales, E. Tutuc, I. Brener, and G. Shvets, Nat. Commun. **5**, 3892 (2014).
[7] A. Zhan, S. Colburn, R. Trivedi, C. Dodson, and A. Majumdar, ACS Photon. **3**, 209 (2016).
[8] C. Pfeiffer and A. Grbic, Phys. Rev. Lett. **110**, 197401 (2013).
[9] A. Pors and S. I. Bozhevolnyi, Opt. Express **21**, 27438 (2013).
[10] D. Lin, P. Fan, E. Hasman, and M. L. Brongersma, Science **345**, 298 (2014).
[11] E. Karimi, S. A. Schulz, I. De Leon, H. Qassim, J. Upham, and R. W. Boyd, Light Sci. Appl. **3**, e167 (2014).
[12] A. Arbabi, Y. Horie, M. Bagheri, and A. Faraon, Nat. Nanotechnol. **10**, 937 (2015).
[13] D. Veksler, E. Maguid, N. Shitrit, D. Ozeri, V. Kleiner, and E. Hasman, ACS Photon. **2**, 661 (2015).
[14] E. Maguid, I. Yulevich, D. Veksler, V. Kleiner, M. Brongersma, and E. Hasman, Science **352**, 1202 (2016).
[15] H. J. Rance, T. J. Constant, A. P. Hibbins, and J. R. Sambles, Phys. Rev. B **86**, 125144 (2012).
[16] N. Shitrit, I. Yulevich, E. Maguid, D. Ozeri, D. Veksler, V. Kleiner, and E. Hasman, Science **340**, 724 (2013).
[17] E. Martini, M. Mencagli, and S. Maci, Philos. Trans. R. Soc. London A **373**, 20140355 (2015).
[18] Y. B. Li, B. G. Cai, X. Wan, and T. J. Cui, Opt. Lett. **39**, 5888 (2014).
[19] A. Vakil and N. Engheta, Science **332**, 1291 (2007).
[20] A. High, A. D. R. C. Devlin, M. Polking, D. Wild, J. Perczel, N. P. de Leon, M. Lukin, and H. Park, Nature (London) **522**, 192 (2015).
[21] J. S. Gomez-Diaz, M. Tymchenko, and A. Alù, Phys. Rev. Lett. **114**, 233901 (2015).
[22] O. Y. Yermakov, A. I. Ovcharenko, M. Song, A. A. Bogdanov, I. V. Iorsh, and Y. S. Kivshar, Phys. Rev. B **91**, 235423 (2015).
[23] I. Trushkov and I. Iorsh, Phys. Rev. B **92**, 045305 (2015).
[24] A. Nemilentsau, T. Low, and G. Hanson, Phys. Rev. Lett. **116**, 066804 (2016).
[25] F. Rodriguez-Fortuno, G. Marino, P. Ginzburg, D. OConnor, A. Martinez, G. Wurtz, and A. Zayats, Science **340**, 328 (2013).
[26] K. Y. Bliokh and F. Nori, Phys. Rep. **592**, 1 (2015).
[27] A. Aiello, P. Banzer, M. Neugebauer, and G. Leuchs, Nat. Photon. **9**, 789 (2015).
[28] J. Petersen, J. Volz, and A. Rauschenbeutel, Science **346**, 67 (2014).
[29] B. le Feber, N. Rotenberg, and L. Kuipers, Nat. Commun. **6**, 6695 (2015).
[30] I. Söllner, S. Mahmoodian, S. L. Hansen, L. Midolo, A. Javadi, G. Kiršanskė, T. Pregnolato, H. El-Ella, E. H. Lee, J. D. Song, S. Stobe, and P. Lodahl, Nat. Nanotechnol. **10**, 775 (2015).
[31] K. Y. Bliokh, D. Smirnova, and F. Nori, Science **348**, 1448 (2015).
[32] K. Y. Bliokh and F. Nori, Phys. Rev. A **85**, 061801(R) (2012).
[33] K. Y. Bliokh, A. Y. Bekshaev, and F. Nori, Nat. Commun. **5**, 3300 (2014).
[34] A. Gloppe, P. Verlot, E. Dupont-Ferrier, A. Siria, P. Poncharal, G. Bachelier, P. Vincent, and O. Arcizet, Nat. Nanotechnol. **9**, 920 (2014).

[35] L. P. Neukirch, E. von Haartman, J. M. Rosenholm, and A. N. Vamivakas, Nat. Photon. **9**, 653 (2015).
[36] A. Canaguier-Durand, A. Cuche, C. Genet, and T. W. Ebbesen, Phys. Rev. A **88**, 033831 (2013).
[37] A. Canaguier-Durand and C. Genet, Phys. Rev. A **89**, 033841 (2014).
[38] V. I. Belotelov and A. K. Zvezdin, Phys. Rev. B **86**, 155133 (2012).
[39] K. Bliokh, F. Rodriguez-Fortuno, F. Nori, and A. Zayats, Nat. Photon. **9**, 796 (2015).
[40] J. D. Caldwell, A. V. Kretinin, Y. Chen, V. Giannini, M. M. Fogler, Y. Francescato, C. T. Ellis, J. G. Tischler, C. R. Woods, A. J. Giles, M. Hong, K. Watanabe, T. Taniguchi, S. A. Maier, and K. S. Novoselov, Nat. Commun. **5**, 5221 (2014).
[41] P. Li, M. Lewin, A. V. Kretinin, J. D. Caldwell, K. S. Novoselov, T. Taniguchi, K. Watanabe, F. Gaussmann, and T. Taubner, Nat. Commun. **6**, 7507 (2015).
[42] S. Dai, Q. Ma, T. Andersen, A. Mcleod, Z. Fei, M. Liu, M. Wagner, K. Watanabe, T. Taniguchi, M. Thiemens, F. Keilmann, P. Jarillo-Herrero, M. M. Fogler, and D. N. Basov, Nat. Commun. **6**, 6963 (2015).
[43] Z. Liu, H. Lee, Y. Xiong, C. Sun, and X. Zhang, Science **315**, 1686 (2007).
[44] S. Ishii, A. V. Kildishev, E. Narimanov, V. M. Shalaev, and V. P. Drachev, Laser Photon. Rev. **7**, 265 (2013).
[45] I. V. Iorsh, I. S. Mukhin, I. V. Shadrivov, P. A. Belov, and Y. S. Kivshar, Phys. Rev. B **87**, 075416 (2013).
[46] A. V. Chshelokova, P. V. Kapitanova, A. N. Poddubny, D. S. Filonov, A. P. Slobozhanyuk, Y. S. Kivshar, and P. A. Belov, J. Appl. Phys. **112**, 073116 (2012).
[47] A. Poddubny, I. Iorsh, P. Belov, and Y. Kivshar, Nat. Photon. **7**, 948 (2013).
[48] K. L. Koshelev and A. A. Bogdanov, Phys. Rev. B **92**, 085305 (2015).
[49] M. I. D'yakonov, Sov. Phys. JETP **67**, 714 (1988).
[50] O. Takayama, L.-C. Crasovan, S. K. Johansen, D. Mihalache, D. Artigas, and L. Torner, Electromagnetics **28**, 126 (2008).
[51] K. Y. Bliokh, Y. S. Kivshar, and F. Nori, Phys. Rev. Lett. **113**, 033601 (2014).
[52] M. V. Berry, J. Opt. A Pure Appl. Opt. **11**, 094001 (2009).
[53] S. A. Mikhailov and K. Ziegler, Phys. Rev. Lett. **99**, 016803 (2007).
[54] P. Lodahl, S. Mahmoodian, S. Stobbe, P. Schneeweiss, J. Volz, A. Rauschenbeutel, H. Pichler, and P. Zoller, arXiv:1608.00446.
[55] J. I. Cirac, P. Zoller, H. J. Kimble, and H. Mabuchi, Phys. Rev. Lett. **78**, 3221 (1997).
[56] D. Lu, J. D. Biamonte, J. Li, H. Li, T. H. Johnson, V. Bergholm, M. Faccin, Z. Zimborás, R. Laflamme, J. Baugh, and S. Lloyd, Phys. Rev. A **93**, 042302 (2016).
[57] F. Cardano and L. Marrucci, Nat. Photon. **9**, 776 (2015).